

Metal Foils for Bipolar Plates—Correlation of Initial Grain Size and Forming Behavior of 316L



Alexander Bauer, Thomas Mehner, Birgit Awiszus, and Thomas Lampke

Abstract As the forming of metallic bipolar plates is mostly still in the state of research, the underlying forming mechanisms are not fully understood. This study deals with the topic of different grain sizes in the initial metal sheets and their influence on the forming results. Therefore, a work-hardened 316L-foil (0.1 mm) was processed with different heat treatment strategies resulting in three different grain sizes with average grain diameters of 47.4, 19.3, and 7.9 μm . Afterward, all heat-treated blanks were cut and deep-drawn between two rigid dies to form a bipolar plate flow field. Besides force and geometrical factors like thinning and springback, the microstructure was analyzed by XRD and EBSD. Using these characterization methods, the mechanisms of twinning and preferred deformation of specific grain orientations during the forming process can be identified. Therefore, the impact of size effects on the forming behavior of metallic bipolar plates is shown. It can be concluded that a fine-grained initial state is preferable.

Keywords Bipolar plates · Microstructure · Forming · 316L

1 Introduction

Metallic bipolar plates for Proton-Exchange Membrane (PEM) fuel cells are a promising component in the context of relevant topics like resource efficiency and the reduction of emissions in the mobility sector. An application of metallic bipolar plates can significantly reduce manufacturing costs and therefore help the PEM fuel cell to achieve a widespread market penetration in general. Nevertheless, the mass

A. Bauer (✉) · B. Awiszus

Faculty of Mechanical Engineering, Virtual Production Engineering, Chemnitz University of Technology, Institute of Machine Tools and Production Processes, Reichenhainer Straße 70, 09126 Chemnitz, Germany
e-mail: a.bauer@mb.tu-chemnitz.de

T. Mehner · T. Lampke

Materials and Surface Engineering, Faculty of Mechanical Engineering, Chemnitz University of Technology, Institute of Materials Science and Engineering, Erfenschlager Straße 73, 09125 Chemnitz, Germany

© The Minerals, Metals & Materials Society 2021

G. Daehn et al. (eds.), *Forming the Future*, The Minerals, Metals & Materials Series, https://doi.org/10.1007/978-3-030-75381-8_146

1743

production of metallic bipolar plates is still being researched. One reason for that is the underlying forming mechanisms of metal foils, which are not easily scaled down from conventional thicknesses to thicknesses of 0.5 mm. The related size effects, which cause these kinds of differences, were analyzed in several publications. *Tiesler et al.* provide a good overview about the size effects that occur in deep-drawing processes, for instance, the increasing influence of single grains [1]. For a comparison of metal sheets (thicknesses > 1 mm) with the corresponding metal foils (<25 μm) of aluminum and unalloyed steel, it was found that the friction values increased during the forming of the metal foils, while the limited drawing ratio decreased [2]. Other scientists found out that the anisotropy values decreased and the yield strength as well as the tensile strength increased with a rising number of grains over the sheet thickness of 0.1 mm in 1.4301 stainless steel foils [3, 4]. Several other publications also dealt with the appearance of size effects during the forming of copper foils [5, 6] or aluminum [7, 8]. In general, it can be seen that the particular forming mechanisms of metal foils are mostly analyzed separately and without a special focus such as the use as a bipolar plate. In this article, the relevant effects are analyzed concerning the requirements for bipolar plates. Therefore, three different grain sizes, which were generated from the initial metal foils and which were subsequently formed to bipolar plate-shaped test samples, were analyzed. Besides general methods for the analysis of the macro- and microscopical geometry development, X-ray diffraction (XRD), and electron backscatter diffraction (EBSD) were used to achieve an in-depth understanding of the microstructural phenomena, which appear during the forming process. On the one hand, this leads to better insights into the forming process and the parameters that affect it. On the other hand, the knowledge gained from this research results in a recommendation of an initial state of the metal foils which differs from those currently used for the majority of semi-finished products for metallic bipolar plates.

2 Materials and Methods

The initial material was a conventional 316L (1.4404) stainless steel foil with a thickness of 0.1 mm in a work-hardened state. The chemical composition (mass fraction) is specified as follows: C: 0.02%; Si: 0.41%; Mn: 1.34%; P: 0.03%; S: 0.004%; Cr: 16.64%; Ni: 10.01%; Mo: 2.00%. The tensile strength was 1274 MPa, which is an increase of about 85% compared to the annealed material state. In preparation for the heat treatments, the samples were cut from the coil with a stationary precision cutting machine to a size of 80 mm \times 50 mm. Afterward, the cut samples were heat-treated in a *Torvac 12 Mark IV* vacuum furnace. The required temperatures in order to achieve three significantly different grain sizes were obtained from preliminary investigations (Table 1).

Subsequent to the holding times from Table 1, the samples were slowly cooled down to room temperature within the furnace, under vacuum condition, and without additional coolants.

Table 1 Different grain sizes with associated heat treatment parameters

Requested grain size	Nomenclature	Temperature (°C)	Duration (h)
Coarse (≈50 μm)	316L-CG	1100	0.5
Medium (≈25 μm)	316L-MG	970	1
Fine (≈7.5 μm)	316L-FG	850	1

After the heat treatment, four specimens of each material state (316L-CG, -MG, -FG) were formed within a four-column servo press (*Hegewald & Peschke Meß- und Prüftechnik GmbH*) (Fig. 1a). This forming machine, which is specialized in performing microforming operations with high accuracy, enabled a precise forming process with an identical start at a pre-force of 150 N, a velocity of 1 mm/s, and a defined stop at a drawing gap of 0.12 mm. This gap was combined from the sheet thickness (0.1 mm) and an additional offset (0.02 mm). No additional lubrication was used. The geometry was defined by a rigid punch and a rigid die with the shape of relevant bipolar plate channel geometries and a circumferential outer structure (Fig. 1b, c). Figure 1c shows the relevant channel dimensions: RE: entry radius, RG: ground radius, BW: bottom width, FA: flank angle, and h: channel height.

Subsequent to the forming operation, a variety of evaluation methods was used to examine the results. First of all, the geometry evolution was analyzed on the macro- and microscale. The macroscale investigations were carried out with a photogrammetric *GOM ATOS Core* system, which digitized the formed 3D geometry and enabled a separate evaluation with a direct comparison of the CAD or FEM geometry in the software tool *GOM Inspect* (Fig. 2 left, middle). For this comparison, four spots on the edge of the flow field were defined at first. In the second step, the perpendicular distance between the experimental GOM geometry and the CAD or FEM result was measured to determine the differences in the geometrical development.

The channel thinning was analyzed with micrographs from the channel cross sections under an optical microscope. Therefore, the samples were prepared with a

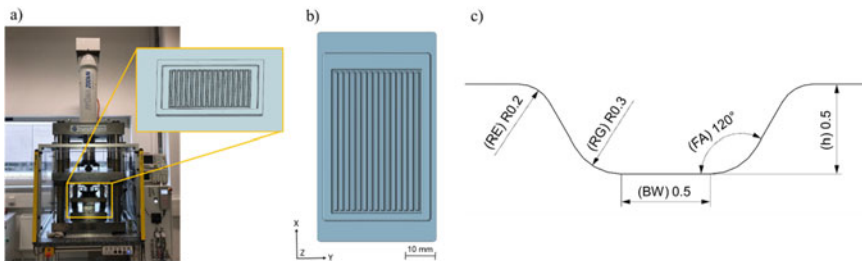


Fig. 1 Left: Servo press with enlarged CAD-surface of die [9]; middle: top view of a test sample [9]; right: channel cross section of a test sample [according to 10]. (Color figure online)

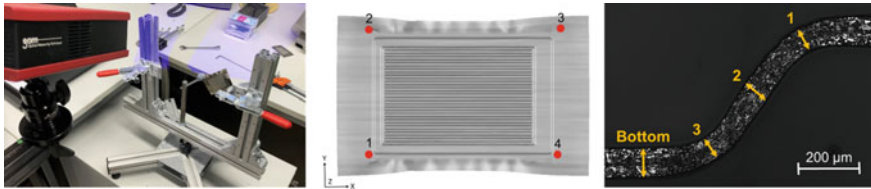


Fig. 2 Left: GOM measurement; middle: arrangement of measurement positions for comparison of the macroscopic geometry; right: arrangement of measurement positions for thinning. (Color figure online)

Discotom cutting machine transversal to the channels, embedded in epoxy resin, and subsequently polished and etched to show microstructural features. Afterward, the specimens were analyzed under an *Axiovert 200* microscope with the corresponding software *AxioVision*, both from the *Carl Zeiss AG*. The results were averaged from three different channels in the middle of the flow fields. Furthermore, four different spots were measured for each channel: upper radius, flank, lower radius, and bottom (Fig. 2 right).

Furthermore, the roughness was evaluated with a *VK-X1000* confocal microscope from the *Keyence Corporation*. The measurements by focus variation were implemented at an area of $5.5 \text{ mm} \times 4.5 \text{ mm}$ and consecutively examined within the *Keyence Multi-File-Analyzer* software. Therefore, multiple measuring sections were defined at the channel top, the flank, and the channel bottom and afterwards combined to a mean value.

To achieve a deeper understanding of the microstructural phenomena like twinning and grain orientation dependent deformation, EBSD was used. The experiments were conducted in a *Neon 40EsB* scanning electron microscope of the *Carl Zeiss AG* using a voltage of 15 kV and a sample tilt of 70° . The step size was $0.1 \text{ } \mu\text{m}$. For the evaluation, the software *TEAM EBSD Analysis System (EDAX Inc.)* was used. A cleanup has been performed using Grain Confidence Index Standardization (tolerance angle 15°) and Neighbor Confidence Index Correlation (minimum confidence index of 0.2). All of the EBSD images were taken from the upper radius area as one of the spots, which is affected the most by the forming process (Fig. 3).

Further investigations of the microstructure were done by XRD using a diffractometer *D8 Discover (Bruker AXS)* with $\text{Co K}\alpha$ radiation (tube parameters: 40 kV,

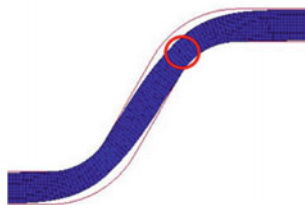


Fig. 3 Position of the EBSD measurements (red mark). (Color figure online)

40 mA), polycap optics for beam focusing, a pinhole aperture with a diameter of 0.5 mm, and an energy-filtered 1D detector Lynxeye XE. A step size of 0.02° with a measurement time of 7.2 s/step. Microstrains (peak broadening caused by lattice defects) and crystallite sizes were evaluated using the program *TOPAS* (*Bruker AXS*).

3 Results and Discussion

3.1 Heat Treatments of the Metal Foils

The 316L stainless steel foil was used in a work-hardened state to enable recrystallization with a broad spectrum of possible grain sizes (Fig. 4). Besides the average grain diameter (316L-CG: $47.4 \mu\text{m}$; 316L-MG: $19.3 \mu\text{m}$; 316L-FG: $7.9 \mu\text{m}$), the micro-sections of all different grain sizes show the presence of crystal twins. One reason for the occurrence of the crystal twins in face-centered cubic materials is the tendency to develop twins during annealing processes [11]. On the one hand, a higher amount of annealing twins can be seen in the fine-grained specimen (316L-FG) due to its smaller grain sizes. On the other hand, the ratio of the total length of the boundaries of crystal twins to the total length of grain boundaries in general is lower in the fine-grained specimen (316L-FG) than in the coarse-grained specimen (316L-CG). This implies that the impact of the twins on the forming behavior, as a possible boundary for the accumulation of dislocations, has to be analyzed based on forming experiments. All forming-relevant mechanical properties, like flow and forming limit curves, were affected by the heat treatments. This has previously been discussed by the authors [9].

For comparison, a work-hardened and an annealed state of 316L foil were measured by XRD to analyze the amount of dislocations (i.e., microstrains, which are directly connected to the presence of dislocations). The measured microstrain of the work-hardened state was 0.47, in contrast to the annealed state, for which the microstrain is below the detection limit. According to the measured values, the investigated samples showed a complete recrystallization after the heat treatments with the temperatures given in Table 1.

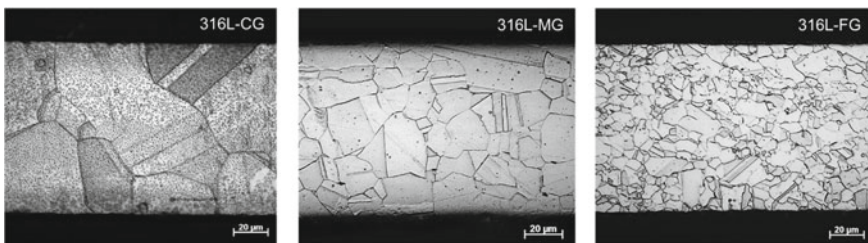


Fig. 4 Microsections of 316L with different heat treatment temperatures

3.2 Forming Experiments

All specimens were intentionally formed without a binder (blank holder) to show the impact on the forming results more clearly and unaffected by additional material flow controlling technologies (Fig. 5). A comparison of the required forming forces between the samples of different grain sizes showed no significant differences. Therefore, it is not discussed in more detail within this publication. In general, the sheets of all grain sizes reached the final shape at approximately 90 kN.

At first sight, it can be directly seen that the three grain sizes show different values for the distortion caused by the springback of the samples. The springback of the coarse-grained specimens (316L-CG) is the lowest, whereas for 316L-MG and 316L-FG, it is almost identical. This classification can be confirmed in the photogrammetric analyses. The coarse-grained specimens show the lowest perpendicular deviation between the experimental geometry and the CAD construction (Fig. 6). The wrinkles in all specimens appear as the reason for the stresses connected with the material flow into the die.

The corresponding values of all samples can be found in Table 2.

Regarding the detected springback effect and the related accuracy of the forming result, the coarse-grained specimens show the best values for a forming process without binder. As the macrostructural development of the geometry is just one factor which has to be considered for a comparison of initial material states. Further aspects have to be examined for a reliable statement.

The thinning behavior of the three grain sizes is shown in Table 3. The fine-grained and the middle-grained specimens look almost identical in regards to the thinning.

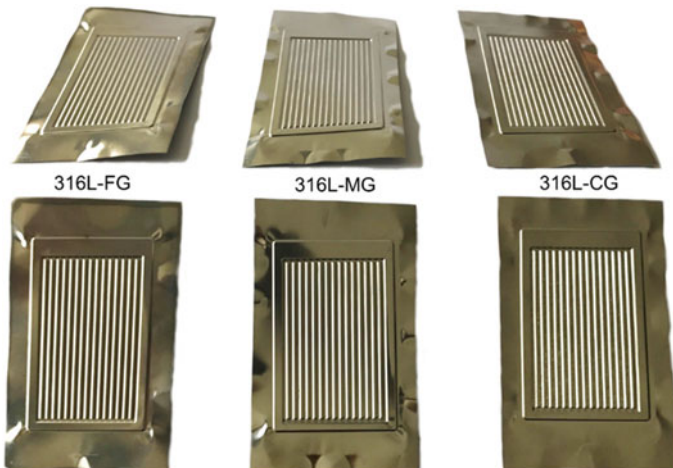


Fig. 5 Forming results for different heat-treatment temperatures and without binder. (Color figure online)

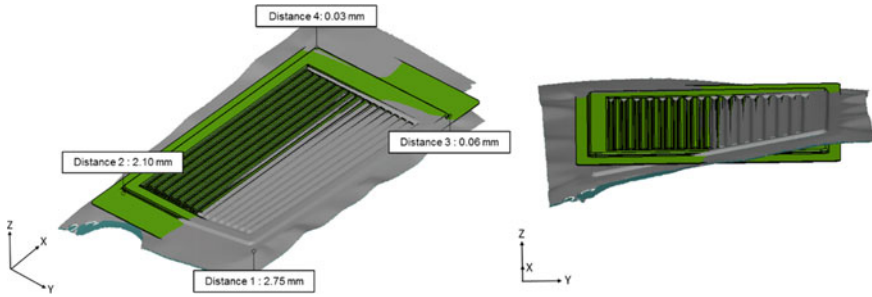


Fig. 6 Differences of 316L-MG between CAD geometry (green) and experimental forming results (gray). (Color figure online)

Table 2 Comparison of the distances between experiments and CAD construction

Measuring point	Deviations forming versus CAD (mm)		
	316L-CG	316L-MG	316L-FG
Distance 1	+1.75	+2.75	+3.20
Distance 2	-1.32	-2.10	-2.10
Distance 3	-0.02	-0.06	-0.04
Distance 4	+0.06	+0.03	+0.07

Table 3 Comparison of the thinning in the formed specimens with different gain sizes

Measuring point	316L-CG	316L-MG	316L-FG
Bottom, reference value (μm)	98.9	96.1	98.2
	Thinning (%)		
1. Channel top radius	23.5	23.0	25.4
2. Flank	20.0	13.4	14.6
3. Channel bottom radius	23.1	19.0	21.8

The greatest difference can be seen in the coarse-grained specimen, which shows a more uniform thinning, even in the channel flanks.

The coarse-grained specimens show excess thinning effects in a few channel flanks over the whole specimen, which is not considered in the mean values of Table 3. An example is shown in Fig. 7.

For comparability, these exceptional cases were not considered for the values in Table 3 as only just a few channels were affected by this exaggerated thinning, but in terms of the microstructural effects, these cases are of special interest. The otherwise similar values of the thinning require an in-depth investigation in order to understand the additional effects caused by the forming and their influence on the future application in fuel cells. Thus, the measurements of the thinning were directly correlated to the results from the EBSD. The differences in the material-flow behavior

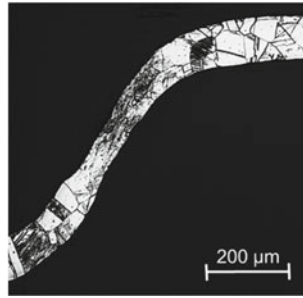


Fig. 7 Example for excess thinning in the channel flanks of 316L-CG

and the grain structure result from the specific microstructure of the specimens with different grain sizes.

During the analysis of the medium grain sizes, the annealing twins, which were caused by the heat treatment, were still clearly visible (Fig. 8, left). Most of them can be seen for orientations close to $\{111\}$ (blue, violet) or $\{001\}$ (red, orange). The right image of Fig. 8 shows the forming twins as well as the annealing twins with red lines. The formation of forming twins is related to energetic reasons. While crystallographic slipping is the main forming mechanism, which appears in ductile materials, plastic deformation can also be enabled by twinning [12]. In the length measurements of the grain and twin boundaries in all measured grains, almost identical values can be measured for both boundary types (total length grain boundaries: 4.40 mm; total length twin boundaries: 4.47 mm). However, not all of the twin boundaries could be

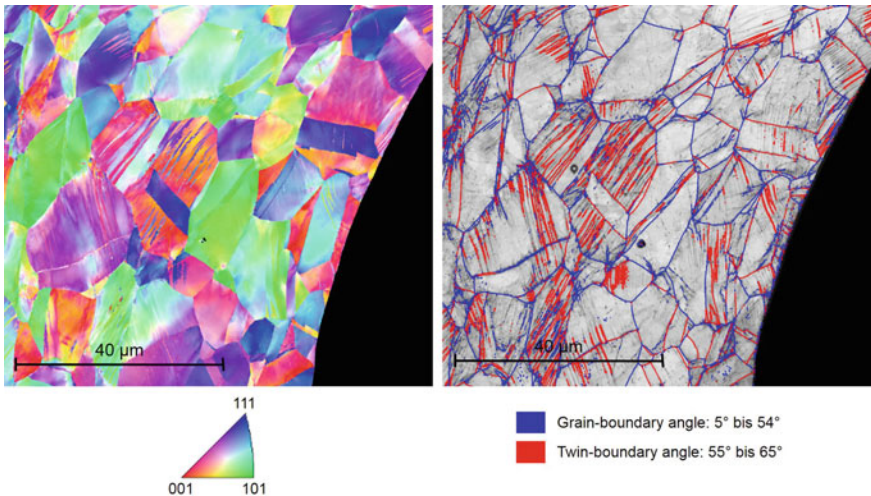


Fig. 8 EBSD micrographs of formed 316L-MG, left: grain orientation (inverse pole figure), right: grain (blue), and twin (red) boundaries. (Color figure online)

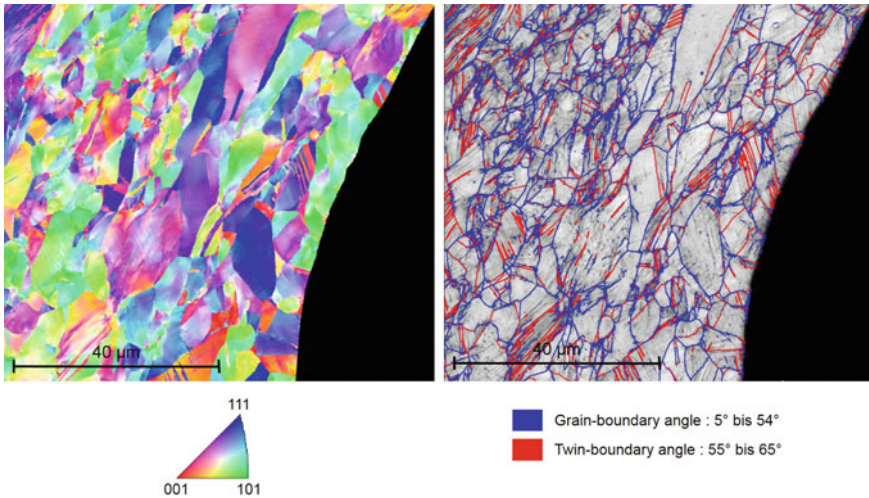


Fig. 9 EBSD micrographs of formed 316L-FG, left: grain orientation (inverse pole figure), right: grain (blue), and twin (red) boundaries. (Color figure online)

analyzed due to their small width and the limited resolution of EBSD. With a closer analysis of Fig. 8, the annealing twins can still be observed by their characteristic straight boundaries. In the left image, the forming twins can be identified as sharp, wide bands within the grains.

The evaluation of the EBSD image of a 316L-FG specimen showed a similar deformation as seen in 316L-MG, as there exists a variety of grain boundaries (Fig. 9). Therefore, a homogenous deformation is possible for the medium as well as for the fine-grained sizes (Table 3). Further refinement of the grain size would not change the thinning significantly.

In a direct comparison between 316L-FG and 316L-MG, it can be seen that the fine-grained specimen developed less forming twins. The total length of all grain boundaries comes to 6.55 mm, whereas the twin-boundary length just reached a total of 3.85 mm. This means that the summed-up length of grain boundaries is nearly twice as large as for the twin boundaries, while the ratio within the medium grain sizes was almost equivalent. The reason is the higher number of possible slip planes in the fine-grained specimen, which is more favorable for the forming mechanisms from the energetic point of view. This means that the size effects have a higher impact on the forming mechanisms with a decreasing amount of grains over the thickness of the specimen. In particular, this can be seen most clearly for the coarse-grained specimen 316L-CG (Fig. 10).

The microsections in Fig. 7 already showed that some of the flanks within the 316L-CG samples underwent an excess thinning. One reason for this material behavior is that some areas of the 316L-CG samples are only one or two grains thick. This means that in parts of the sample there is no possibility for crystallographic slipping, which results in a significant stretching of single grains and thus

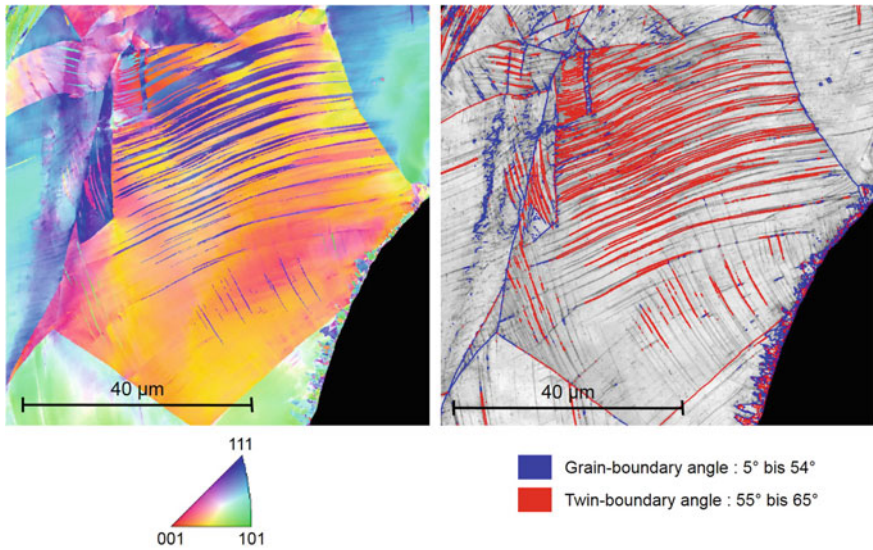


Fig. 10 EBSD micrographs of formed 316L-CG, left: grain orientation (inverse pole figure), right: grain (blue), and twin (red) boundaries. (Color figure online)

unwanted thinning in formed areas. Such a material behavior can also be referred to as a size effect, which means that there are changes in the plasticity between highly fine-grained materials and local areas with fewer grains over the specimen's thickness. This can also be concluded from the EBSD analysis in Fig. 10. The total amount of crystal twins, which occur during the forming process, are more than double the length as the grain boundaries (total length of grain boundaries: 2.34 mm; total length of twin boundaries: 5.07 mm; some very thin twin boundaries are not included). This implies that the samples lack slipping planes and therefore crystal twinning became the major forming mechanism. In combination with the presence of only one or two single grains across the thickness, this leads to increased thinning effects.

Concluding the analyses of the thinning behavior and the crystallographic effects, the fine-grained specimens show the best attributes for the use as a bipolar plate. A clearly polycrystalline microstructure enables good forming behavior and the highest forming capacity without unpredictable thinning or damage. The total length of 10.40 mm for grain and twin boundaries is the highest value of the investigated specimens, which indicates that 316L-FG contains the longest boundaries to accumulate dislocations. This means that the fine-grained structures have a higher stability against external deformation.

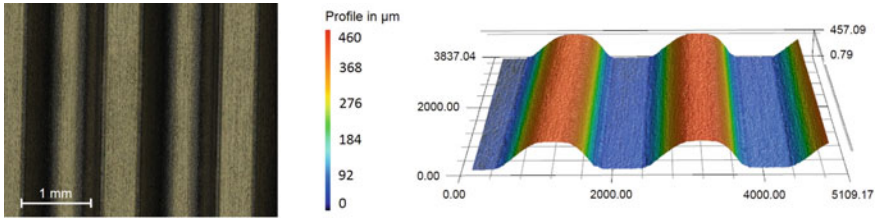


Fig. 11 Confocal measurements of a formed specimen (316L-FG), left: scanned area, right: sample profile. (Color figure online)

Table 4 Arithmetical mean deviation (R_a) values of formed samples with different initial grain sizes

Measuring position	Arithmetical mean deviation R_a (μm)		
	316L-CG	316L-MG	316L-FG
Channel top	3.69	3.25	3.21
Flank	6.25	4.10	3.68
Channel bottom	3.64	2.89	2.03

3.3 Roughness

For metallic bipolar plates, roughness is an important factor during the operational cycles with a flowing medium and the corrosive environment. Therefore, the evolution of the roughness that results from the forming processes with different initial grain sizes is important. The roughness of the initial metal foils prior to the heat treatments was measured with $R_a = 3.2 \mu\text{m}$. With a focus on the roughness, of the heat-treated and formed specimen, at the channel top, the flank, and the channel bottom, distinct differences can be observed between the three sample types. Figure 11 shows the measured area from the fine-grained formed specimen and the corresponding profile.

All measured values are summarized in Table 4.

From the measured values in Table 4, different conclusions can be drawn. Firstly, it is visible that all specimens reached the highest roughness values in the flank areas, which also include the radii. From the forming point of view, this is an expected behavior because in areas with free strain, the surface is enlarged, which in turn causes an increase in roughness [13]. The highest loads for the forming of these bipolar plate channel structures can be found in the radii and flank areas. Additionally, the different initial grain sizes can be seen to have an effect. The highest roughness values can clearly be observed in the coarse-grained material and the lowest ones were measured in the fine-grained samples. For that reason, it can be concluded that the initial grain size has a major impact on the development of the surface roughness after the forming process. This is of special interest for future use as a bipolar plate. A higher roughness provides a bigger surface for corrosion while the accumulation of produced water in pits or gaps is supported by bigger grains. This can lead to the formation of local elements where the corrosive attack starts. With respect to the

durability of the bipolar plates, fine-grained specimens would be preferable due to the lower roughness after forming.

4 Conclusions

In summary, it can be clearly seen that different grain sizes in the semi-finished products lead to considerable differences in the forming results, which occur due to size effects. For the definition of an ideal initial material state, the results are contrary. The coarse-grained specimens showed the lowest springback for a forming without binder, which would be preferable. However, the fine-grained specimens showed the best microstructural properties with regard to the application as a bipolar plate in PEM fuel cells. With a view on the roughness evolution, the best results were achieved by the fine-grained material, which could reduce corrosion during the operation of the fuel cell.

Another argument, which supports the use of fine-grained specimens, can be found in the production technology. In the specific case of deep drawing of metallic bipolar plates, a binder can be added to the tool design. An optimization of this process, which was used in the experiments presented, showed that the springback effect, which occurred in different intensities depending on the grain size, was almost eliminated (Fig. 12).

Within Fig. 12, it is clearly visible that, when compared to Fig. 5, no springback and no differences between the different grain sizes can be observed. This means

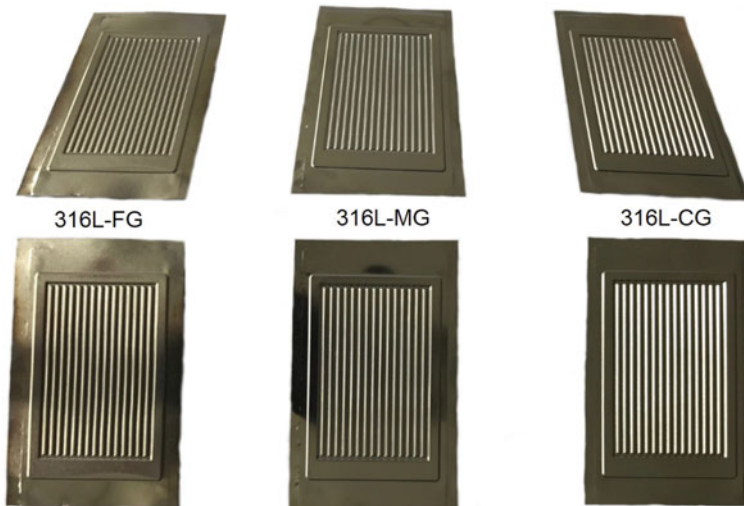


Fig. 12 Optimized forming results for different heat treatment temperatures and with binder. (Color figure online)

that the fine-grained specimen, which led to the highest springback effect without a binder, also gave flat results without wrinkles. Thus, it can be seen that even the worst springback effect of the fine-grained specimen was successfully compensated by technological adaption.

Furthermore, considering the production costs, a fine-grained microstructure could be produced with a low annealing temperature after the last rolling pass. In the present case, the fine-grained specimens were annealed at a temperature of 850 °C, whereas conventional heat treatments were done at around 1000 °C for medium grain sizes. The production of coils of fine-grained material is more resource- and cost-efficient. Overall, based on the results of this investigation, the fine-grained initial state (grain diameter < 10 μm) can be recommended for the production of metallic bipolar plates.

Within modern engineering product or process developments, the use of numerical simulations like FEM is a conventional strategy to predict requested results. The FEM simulation of metal foil forming processes is challenging because of the appearance of size effects like mentioned in this paper. Nevertheless, numerical simulations were done to predict the forming results even with different initial material states and grain sizes. The results with the specific material data like flow curve, anisotropy values, and forming limit curve showed a very good agreement with the experiments, especially compared with conventional 316-L database materials. An associated research project will be described in more detail in upcoming publications.

Acknowledgments The authors gratefully acknowledge the support by the colleagues at Chemnitz University of Technology from the Micromanufacturing Technology group for providing access to the servo press as well as from the Forming and Joining group for providing access to the GOM ARGUS system. The authors thank Steffen Clauß for performing the EBSD measurements and Morgan Uland for English proofreading.

References

1. Tiesler N, Engel U, Geiger M (1999) Forming of microparts—effects of miniaturization on friction. In: Proceedings of the 6th ICTP, 19–24 September, S 889–894
2. Vollertsen F, Hu Z, Schulze Niehoff H, Theiler C (2004) State of the art in micro forming and investigations into micro deep drawing. *J Mater Process Technol* 151:70–79
3. Chen C-H, Gau J-T, Lee R-S (2009) An experimental and analytical study on the limit drawing ratio of stainless steel 304 foils for microsheet forming. *Mater Manuf Process* 24:1256–1265
4. Lee RS, Chen CH, Gau JT (2008) Effect of thickness to grain size ratio on drawability for micro deep drawing of AISI 304 stainless steel. In: Conference presentation: 9th international conference on technology of plasticity, ICTP, S 183–188
5. Chan WL, Fu MW (2012) Experimental and simulation based study on micro-scaled sheet metal deformation behavior in microembossing process. *Mater Sci Eng A* 556:60–67
6. Fu MW, Yang B, Chan WL (2013) Experimental and simulation studies of micro blanking and deep drawing compound process using copper sheet. *J Mater Process Technol* 213:101–110
7. Hu Z, Wielage H, Vollertsen F (2011) Forming behavior of thin foils. *Key Eng Mater* 473:1008–1015

8. Brabie G, Costache EM, Nanu N, Chirita B (2013) Prediction of minimization of sheet thickness variation during deep drawing of micro/milli parts. *Int J Mech Sci* 68:277–290
9. Bauer A, Graf M, Härtel S, Awiszus B (2018) Investigations on the optimization of the initial state for the forming process of metallic bipolar plates. In: Conference presentation: 21st international conference on advances in materials & processing technologies, Dublin City University, Ireland
10. Bauer A, Härtel S, Awiszus B (2019) Manufacturing of metallic bipolar plate channels by rolling. *Jo Manuf Mater Process* 3:48
11. Kauffmann A (2014) Gefügeverfeinerung durch mechanische Zwillingsbildung in Kupfer und Kupfermischkristalllegierungen. PhD thesis, Technische Universität Dresden
12. Choi WS (2018) Deformation mechanisms and the role of interfaces in face-centered cubic Fe-Mn-C micro-pillars. RWTH Aachen University, PhD thesis
13. Lötsch K, Jendras P, Härtel S, von Unwerth T (2017) Gestaltanforderungen bei metallischen Bipolarplatten in PEM-Brennstoffzellen. In: XIV. international colloquium on surfaces—proceedings, S 41–51